

Optimality of nonconservative driving for finite-time processes with discrete statesBenedikt Remlein and Udo Seifert *II. Institut für Theoretische Physik, Universität Stuttgart, 70550 Stuttgart, Germany*

(Received 11 March 2021; accepted 11 May 2021; published 28 May 2021)

An optimal finite-time process drives a given initial distribution to a given final one in a given time at the lowest cost as quantified by total entropy production. We prove that for a system with discrete states this optimal process involves nonconservative driving, i.e., a genuine driving affinity, in contrast to the case of a system with continuous states. In a multicyclic network, the optimal driving affinity is bounded by the number of states within each cycle. If the driving affects forward and backwards rates nonsymmetrically, the bound additionally depends on a structural parameter characterizing this asymmetry.

DOI: [10.1103/PhysRevE.103.L050105](https://doi.org/10.1103/PhysRevE.103.L050105)

In thermodynamics, a finite-time process transforms a given initial state into a given final one in a given finite time. This process is optimal if it comes at the lowest cost, i.e., at the lowest entropy production. The condition of a finite time is crucial since quasistatic processes, which require infinitely slow driving, do not generate entropy at all. For macroscopic systems, such processes have been studied under the label of finite-time thermodynamics [1]. For small systems in contact with a thermal environment and, thus, following a stochastic dynamics, optimal finite-time processes were shown to have an inevitable thermodynamic cost that scales asymptotically, such as the inverse of the allocated time [2,3]. This scaling was later shown to be the exact minimal entropy production for any finite time for an underlying Langevin dynamics [4,5], see also Ref. [6]. For a system with discrete state space undergoing a master equation dynamics, this scaling holds asymptotically as several case studies have shown [7–9]. In the linear response regime, an appealing systematic theory for the optimal driving involves geometric concepts, such as the thermodynamic length [10–15]; see Ref. [16] for a brief review. A complementary aspect of this optimization concerns the derivation of speed limits for transformations between an initial and final distribution [17]. For an effective two-state system, a prominent experimental application of optimal protocols is the minimal cost of erasing a bit in a finite-time extension of the Landauer bound [18–22].

A fundamental distinction for any nonequilibrium process is whether or not the driving is conservative, i.e., whether or not it arises from a time-dependent potential. The former case applies *inter alia* to single molecules manipulated with optical tweezers [23,24], to colloidal particles in time-dependent harmonic or anharmonic traps [25], and to stochastic pumps for which the energy of each state (and potentially the barriers in between) are driven [26–28]. Paradigms for nonconservative driving are colloidal particles driven along static periodic potentials and colloidal particles in shear flow. Biophysical and biochemical processes that are driven by unbalanced chemical reactions, such as the hydrolysis of nucleic acids fall in this class as well [29,30].

Emphasizing this distinction leads to the question whether conservative or nonconservative driving leads to a lower cost for a given initial and final state. In a more technical formulation, the question is whether a time-dependent dynamics whose instantaneous stationary state is Boltzmann-Gibbs-like achieves already minimal entropy production or whether an additional nonconservative contribution, which at a fixed control parameter would lead to a genuine nonequilibrium steady state, can further decrease the cost. For systems with a continuous state space, i.e., for Langevin dynamics, it is known that the optimal protocol involves only conservative forces [5,31–33]. Coming back to the example of a colloidal particle on a ring with periodic boundary conditions this result implies that there is nothing gained by allowing a nonconservative force to act on top of a time-dependent potential.

In this Letter, we address this question for systems with discrete states, i.e., for a master equation dynamics with time-dependent rates. We can build on the work of Muratore-Ginanneschi *et al.* [34] who formulated this optimization problem in terms of control theory without addressing the specific question we are interested in. Since they show that the optimization reduces to the Langevin problem in the continuum limit, one might even expect that the optimal protocol for a discrete state space can be achieved with conservative driving as well. In contrast to the continuous case, however, we will prove that the optimal driving is in fact nonconservative. Furthermore, we will show that for a broad class of systems all cycle affinities, defined precisely below as a quantitative measure of the “nonconservativeness” of the dynamics, remain bounded as a function of the number of states in a cycle during the whole process independent of its duration.

We consider a discrete set of states $\{i\}$ of total number N . A transition between two states (i, j) occurs at a rate $k_{ij}(t)$, which is, in general, time dependent. The probability $p_i(t)$ to find the system at time t in state i evolves according to the master equation,

$$\partial_t p_i(t) = \sum_{j \neq i} [k_{ji}(t)p_j(t) - k_{ij}(t)p_i(t)] \equiv - \sum_{j \neq i} j_{ij}(t), \quad (1)$$

with the net probability current $j_{ij}(t)$ through link (i, j) . We parametrize the transition rates as [34]

$$k_{ij}(t) = \kappa_{ij} e^{A_{ij}(t)/2}, \quad (2)$$

with constant symmetric part $\kappa_{ij} = \kappa_{ji}$, which sets the characteristic timescale for the transition from state i to j and time-dependent antisymmetric $A_{ij}(t) = -A_{ji}(t)$. Throughout the Letter, we measure energies in units of a thermal energy and entropy in units of Boltzmann's constant.

Conservative driving implies that the ratio of forward and backward rates is given by the difference of time-dependent free energies $F_i(t)$ leading to

$$A_{ij}(t) = F_i(t) - F_j(t). \quad (3)$$

In contrast, for nonconservative driving $A_{ij}(t)$ cannot be written as a difference of state functions.

It will be convenient to transform the state densities as $\phi_i(t) \equiv \sqrt{p_i(t)}$ and to introduce the nonequilibrium driving function [34],

$$\varphi_{ij}(t) \equiv A_{ij}(t) + 2[\ln \phi_i(t) - \ln \phi_j(t)], \quad (4)$$

which becomes for conservative driving,

$$\varphi_{ij}(t) = B_i(t) - B_j(t) \quad \text{with} \quad B_i(t) \equiv F_i(t) + 2 \ln \phi_i(t). \quad (5)$$

In this representation, the current along link (i, j) transforms to

$$j_{ij}(t) = 2\kappa_{ij}\phi_i(t)\phi_j(t) \sinh \frac{\varphi_{ij}(t)}{2}, \quad (6)$$

and the master equation (1) becomes

$$\partial_t \phi_i(t) = - \sum_{j \neq i} \kappa_{ij} \phi_j(t) \sinh \frac{\varphi_{ij}(t)}{2}. \quad (7)$$

The process that transforms the given initial density $\{\phi_i(0)\}$ to a given final one $\{\phi_i(T)\}$ in time T is optimal if it generates the least overall entropy production,

$$\Delta S_{\text{tot}} \equiv \int_0^T dt \sigma(t), \quad (8)$$

with the entropy production rate [35],

$$\begin{aligned} \sigma(t) &= \sum_{i \neq j} p_i(t) k_{ij}(t) \ln \frac{p_i(t) k_{ij}(t)}{p_j(t) k_{ji}(t)} \\ &= 2 \sum_{i < j} \kappa_{ij} \phi_i(t) \phi_j(t) \varphi_{ij}(t) \sinh \frac{\varphi_{ij}(t)}{2}. \end{aligned} \quad (9)$$

We first show that conservative driving does not lead to minimal entropy production. Assume that within this parameter space (5) we have found the optimal protocol $F_i^*(t)$ leading to $p_i^*(t)$ with currents $j_{ij}^*(t)$. For a unicyclic system, it is then clear that adding a time-dependent $\Delta(t)$ to the clockwise current will still satisfy the master equation (1) and the boundary conditions of a fixed initial and final density. Under the

transformation,

$$j_{ij}(t) \equiv j_{ij}^*(t) + \epsilon_{ij} \Delta(t), \quad (10)$$

with $\epsilon_{ij} = 1 = -\epsilon_{ji}$ for $i < j$ the entropy production rates $\sigma^*(t)$, respectively, $\sigma(t)$, become by a Taylor expansion,

$$\sigma(t) - \sigma^*(t) = \Delta(t) 2 \sum_{i < j} \tanh \frac{B_i^*(t) - B_j^*(t)}{2} + O[\Delta(t)^2]. \quad (11)$$

Since, in general, the linear term will not vanish, see the Supplemental Material [36], we get that the total entropy production found within conservative driving can be further decreased by adding a nonconservative term accounting for such a $\Delta(t)$. Specifically, we can choose $\Delta(t) = \text{const} \neq 0$ such that

$$2\Delta \int_0^T dt \sum_{i < j} \tanh \frac{B_i^*(t) - B_j^*(t)}{2} < 0. \quad (12)$$

This constitutes our first main result: In contrast to the continuous case, optimal protocols for Markov jump processes involve nonconservative driving, i.e., a genuine cycle affinity,

$$\mathcal{A}_c(t) \equiv \sum_{(i,j) \in \mathcal{C}} A_{ij}(t) = \sum_{(i,j) \in \mathcal{C}} \varphi_{ij}(t) \quad (13)$$

for each cycle \mathcal{C} in the network. The above proof can indeed be extended trivially to multicyclic networks since a corresponding $\Delta(t)$ can be added to an arbitrary cycle in which case the summation in (11) is only over the directed links of this cycle.

We next show that all cycle affinities $\mathcal{A}_c(t)$ are bounded by the number of states in each cycle for all times. To do so, we have to derive the Euler-Lagrange equations for the variational problem posed by minimizing the entropy production (8) under the constraints (7) which we add with Lagrangean multipliers $\{\eta_i(t)\}$ that ensure that the densities $\{\phi_i(t)\}$ satisfy the master equation. Thus, we minimize

$$\Delta S \equiv \int_0^T dt L[\{\phi(t), \varphi(t), \eta(t)\}] \quad (14)$$

for given $\{\phi_i(0)\}$ and $\{\phi_i(T)\}$ with the Lagrange function,

$$L(t) \equiv \sigma(t) + \sum_i \eta_i(t) \left[\partial_t \phi_i(t) + \sum_{j \neq i} \kappa_{ij} \phi_j(t) \sinh \frac{\varphi_{ij}(t)}{2} \right]. \quad (15)$$

From $\delta L / \delta \phi_i(t) = 0$, we get the equations of motion for the Lagrange multiplier,

$$\partial_t \eta_i(t) = \sum_{j \neq i} \kappa_{ij} \sinh \frac{\varphi_{ij}(t)}{2} [2\phi_j(t) \varphi_{ij}(t) - \eta_j(t)]. \quad (16)$$

Variation with respect to the protocol $\varphi_{ij}(t)$ leads to

$$\eta_i(t) \phi_j(t) - \eta_j(t) \phi_i(t) = -4\phi_i(t) \phi_j(t) \left[\tanh \frac{\varphi_{ij}(t)}{2} + \frac{\varphi_{ij}(t)}{2} \right]. \quad (17)$$

By summing (17) over an arbitrary cycle with N_c states we get

$$\begin{aligned} 0 &= \sum_{i=1}^{N_c} [\eta_i(t)/\phi_i(t) - \eta_{i+1}(t)/\phi_{i+1}(t)] \\ &= -4 \sum_{i=1}^{N_c} \left[\tanh \frac{\varphi_{i,i+1}(t)}{2} + \frac{\varphi_{i,i+1}(t)}{2} \right], \end{aligned} \quad (18)$$

where we relabeled the neighboring links $(i, j) \in \mathcal{C}$ as $(i, i+1)$. We now use this relation to find for the affinity,

$$\mathcal{A}_c(t) = \sum_{i=1}^{N_c} \varphi_{i,i+1}(t) = -2 \sum_{i=1}^{N_c} \tanh \frac{\varphi_{i,i+1}(t)}{2}, \quad (19)$$

and finally use $|\tanh(x)| \leq 1$ to obtain

$$|\mathcal{A}_c(t)| \leq 2N_c. \quad (20)$$

Thus, for each cycle, the time-dependent affinity is bounded by the number of states within that cycle.

In fact, we can sharpen this bound further to

$$|\mathcal{A}_c(t)| \leq 2(N_c - 2), \quad (21)$$

which is our second main result. Although the formal derivation of this improved bound as shown in the Supplemental Material [36] is somewhat technical, its origin can be understood by the following consideration. Equations (19) and (20) require the affinity and, hence, the sum of the driving functions to be finite, thus, not all $\{\varphi_{ij}(t)\}$ are allowed to tend to, e.g., positive infinity at the same time which was the rationale behind the weaker bound, Eq. (20). At least, one driving function has to compensate this putative divergence by approaching negative infinity. The asymptotic behavior of the affinity is determined by Eq. (18), thus, for all $\varphi_{ij}(t) \rightarrow \pm\infty$ except one that tends to $\varphi_{kl}(t) \rightarrow \mp\infty$, the affinity approaches $\mathcal{A}_c(t) \rightarrow \mp 2(N_c - 2)$.

We now turn to numerics in order to explore how significant the improvement through nonconservative driving is and to check how strong the improved bound (21) is. For a three state system, i.e., $N_c = 3$, we sample arbitrary initial and final distributions and calculate for each pair of them the optimal protocol first for conservative and then for nonconservative drivings. We fix a basic timescale by setting all symmetric prefactors $\kappa_{ij} = \kappa_{ji} = 1$. We find that the nonconservative driving leads to an only minute improvement. For a process transforming the state of the system within a time that is comparable to the intrinsic timescale, i.e., for $T = 1$, the advantage of nonconservative driving is, on average, only on the order of 10^{-5} with a maximal improvement of order 10^{-4} . Even for processes that are ten times faster, i.e., $T = 0.1$, on average, this advantage raises only to 10^{-3} , respectively, 10^{-2} for the maximum value.

The faster the process is, the larger is the maximum affinity applied in the optimal process as shown in Fig. 1. This reflects the fact that a nonequilibrium quantity, such as the cycle affinity, should vanish as the quasistatic limit is approached, i.e., $T \rightarrow \infty$. Although $\mathcal{A}_{\max} \equiv \max_{0 \leq t \leq T} |\mathcal{A}(t)|$ remains below the value of 2 as it should, there are combinations of initial and final densities for which the optimal affinity seems to reach this bound within about 2%. In Fig. 2, we show that

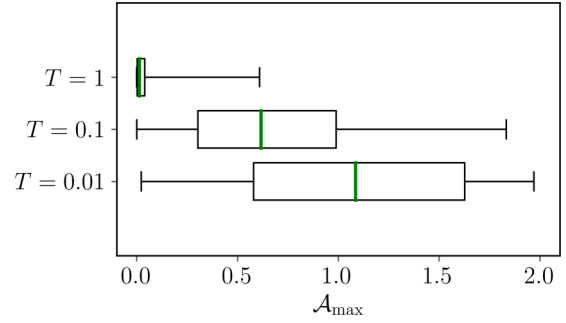


FIG. 1. Influence of the allocated time T on the maximal affinity \mathcal{A}_{\max} for arbitrary sampled initial and final distributions. The edges of the boxes represent the first Q_1 (left) and third quartile Q_3 (right site). The whisker on the left represents the minimum value and on the right the maximum of the data. The thick green line displays the median of the data.

the largest affinities are generated by those initial and final distributions that require to transport either the largest density, i.e., for which $\Delta p_i = p_i(0) - p_i(T)$ is approximately ± 1 for one pair of states or for which $\Delta p_i \simeq 0$ for one state.

Comparing the configurations displayed in Fig. 2, we find that it becomes more difficult to obtain numerically convergent solutions the lower we set the allocated time T . Particularly, we find configurations which tend to transport the largest densities $\Delta p_i \rightarrow \pm 1$ to be numerically unstable (black crosses). At present, it is unclear whether this is due to the numerical scheme, see the Supplemental Material [36] or whether there is a generic problem in the mathematical formulation, e.g., due to diverging derivatives of the driving functions or vanishing probabilities. Another question that remains open is whether there always exist a set of initial and final densities that saturate the bound of the affinity Eq. (21) for a given time T . From our numerical findings we expect that this is the case for configurations that transport the maximal densities, i.e., for $\Delta p_i \simeq \pm 1$. The longer the allocated time T , the closer the transported densities need to be to ± 1 in order to saturate the bound.

So far, with the parametrization (2), we have focused on a symmetric splitting of the driving over each forward and backward rate. In a more general setting, we now allow for a splitting that may be different for each link. We can then parametrize the rates as

$$\begin{aligned} k_{ij} &= \kappa_{ij} \exp(\alpha_{ij} A_{ij}) \\ k_{ji} &= \kappa_{ji} \exp[(1 - \alpha_{ij}) A_{ji}], \end{aligned} \quad (22)$$

with $\kappa_{ij} = \kappa_{ji}$ and one structural parameter for each link given by $0 < \alpha_{ij} = \alpha_{ji} < 1$. Following the derivation in the symmetric case from above, it is straightforward to show that the bound (20) becomes, see the Supplemental Material [36],

$$-\sum_{i=1}^{N_c} \frac{1}{\alpha_{i,i+1}} \leq \mathcal{A}_c \leq \sum_{i=1}^{N_c} \frac{1}{1 - \alpha_{i,i+1}}. \quad (23)$$

If $\alpha_i = 1/2$ for all i , we reproduce Eq. (20).

The more states a cycle has, the larger become our bounds. Naively extrapolating to a cycle with infinitely many states, one might conclude that in such a continuum limit the affinity

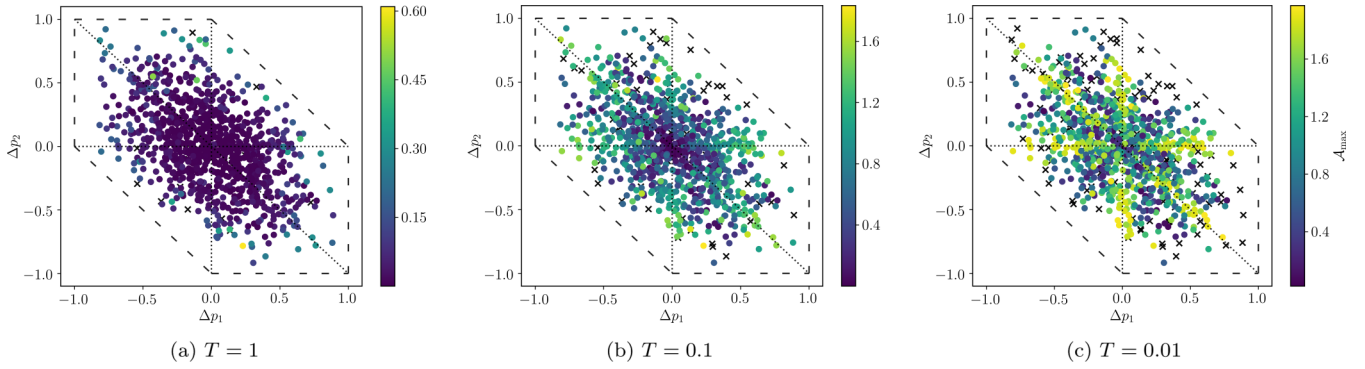


FIG. 2. Influence of the system parameters on the maximal affinity $\mathcal{A}_{\max} \equiv \max_{t \in [0, T]} |\mathcal{A}(t)|$ of arbitrary sampled configurations for different speeds T . $\Delta p_i = p_i(0) - p_i(T)$ displays the change in the state densities. The color bar represents \mathcal{A}_{\max} . The dashed line is defined by $\Delta p_i = \pm 1$ for one i . The dotted line represents $\Delta p_i = 0$ for an i . Black crosses stand for configurations that failed to converge with our algorithm.

could diverge. Such an expectation would be in contrast with the established result that for a Langevin dynamics conservative driving, i.e., zero affinity achieves optimality [5,31]. We finally show that our approach reproduces this continuum limit correctly. Let dx denote a lattice spacing along a cycle. We relabel the driving function of adjacent states in a cycle from $\varphi_{i,i+1}$ to $\varphi_{x,x+dx}$. For small lattice spacing, the affinity becomes

$$\mathcal{A}_c(t) = \sum_{x \in C} \varphi_{x,x+dx}(t) \approx \sum_{x \in C} \varphi'_{x,x}(t) dx \approx \oint_C \varphi'_{x,x}(t) dx, \quad (24)$$

where the prime denotes a derivative with respect to x . Here, we have used that $\varphi_{x,x}(t) = 0$ due to the antisymmetry of $\varphi_{ij}(t)$. Thus, the affinity approaches the contour integral over the spatial derivative of the driving function $\varphi'_{x,x}(t)$ along the cycle. We can calculate the limiting value of this integral by dividing Eq. (18) by -2 and a Taylor expansion, according to

$$0 = \sum_{x \in C} \left[\varphi_{x,x+dx}(t) + 2 \tanh \frac{\varphi_{x,x+dx}(t)}{2} \right] \approx 2 \sum_{x \in C} \varphi'_{x,x}(t) dx \approx 2 \oint_C \varphi'_{x,x}(t) dx. \quad (25)$$

Thus, the cycle affinity indeed has to vanish in the continuum limit. This finding also generalizes to the nonsymmetrical

splitting of the rates Eq. (22), see the Supplemental Material [36].

In conclusion, we have proven that for discrete systems, optimal finite-time processes require nonconservative driving in marked contrast to the case of systems with continuous degrees of freedom. This result implies that with an optimal protocol for the Langevin dynamics, discretizing this solution will, in general, not guarantee optimality over the coarse-grained state space. Furthermore, driving a process, e.g., with unbalanced biochemical reactions, which necessarily imply nonvanishing affinity, can yield lower entropy production than by pumping the system through time-dependent modulations of energies and barriers, which amounts to conservative driving. For each cycle in a multicyclic network, the maximum affinity remains bounded throughout the process, even if the allocated time approaches zero. For driving that affects forward and backward rates symmetrically, the bound depends only on the number of states of a cycle. For a nonsymmetric splitting, a structural parameter enters the bound. Open theoretical problems include a proof of the tightness of the improved bound Eq. (21) for all T and a generalization of this improved bound to asymmetric splitting. For experiments, it remains a challenge to set up a system for which both types of driving, conservative, and nonconservative one, can be implemented and quantitatively be compared with another at the same time.

We thank J. van der Meer and T. Koyuk for stimulating discussions.

- [1] B. Andresen, Current trends in finite-time thermodynamics, *Angew. Chem., Int. Ed.* **50**, 2690 (2011).
- [2] K. Sekimoto and S. Sasa, Complementarity relation for irreversible process derived from stochastic energetics, *J. Phys. Soc. Jpn.* **66**, 3326 (1997).
- [3] T. Schmiedl and U. Seifert, Optimal Finite-Time Processes in Stochastic Thermodynamics, *Phys. Rev. Lett.* **98**, 108301 (2007).

- [4] T. Schmiedl and U. Seifert, Efficiency at maximum power: An analytically solvable model for stochastic heat engines, *Europhys. Lett.* **81**, 20003 (2008).
- [5] E. Aurell, K. Gawedzki, C. Mejía-Monasterio, R. Mohayae, and P. Muratore-Ginanneschi, Refined second law of thermodynamics for fast random processes, *J. Stat. Phys.* **147**, 487 (2012).
- [6] R. Fu, A. Taghvaei, Y. Chen, and T. T. Georgiou, Maximal power output of a stochastic thermodynamic engine, *Automatica* **123**, 109366 (2021).

- [7] M. Esposito, R. Kawai, K. Lindenberg, and C. van den Broeck, Finite time thermodynamics for a single level quantum dot, *Europhys. Lett.* **89**, 20003 (2010).
- [8] G. Diana, G. B. Bagci, and M. Esposito, Finite-time erasing of information stored in fermionic bits, *Phys. Rev. E* **87**, 012111 (2013).
- [9] P. R. Zulkowski and M. R. DeWeese, Optimal finite-time erasure of a classical bit, *Phys. Rev. E* **89**, 052140 (2014).
- [10] G. E. Crooks and C. Jarzynski, Work distribution for the adiabatic compression of a dilute and interacting classical gas, *Phys. Rev. E* **75**, 021116 (2007).
- [11] D. A. Sivak and G. E. Crooks, Thermodynamic Metrics and Optimal Paths, *Phys. Rev. Lett.* **108**, 190602 (2012).
- [12] P. R. Zulkowski, D. A. Sivak, G. E. Crooks, and M. R. DeWeese, Geometry of thermodynamic control, *Phys. Rev. E* **86**, 041148 (2012).
- [13] P. Muratore-Ginanneschi, On the use of stochastic differential geometry for non-equilibrium thermodynamic modeling and control, *J. Phys. A: Math. Theor.* **46**, 275002 (2013).
- [14] P. R. Zulkowski and M. R. DeWeese, Optimal control of overdamped systems, *Phys. Rev. E* **92**, 032117 (2015).
- [15] D. A. Sivak and G. E. Crooks, Thermodynamic geometry of minimum-dissipation driven barrier crossing, *Phys. Rev. E* **94**, 052106 (2016).
- [16] S. Deffner and M. V. S. Bonança, Thermodynamic control—an old paradigm with new applications, *Europhys. Lett.* **131**, 20001 (2020).
- [17] N. Shiraishi, K. Funo, and K. Saito, Speed Limit for Classical Stochastic Processes, *Phys. Rev. Lett.* **121**, 070601 (2018).
- [18] A. Bérut, A. Arakelyan, A. Petrosyan, S. Ciliberto, R. Dillenschneider, and E. Lutz, Experimental verification of Landauer's principle linking information and thermodynamics, *Nature (London)* **483**, 187 (2012).
- [19] Y. Jun, M. Gavrilov, and J. Bechhoefer, High-Precision Test of Landauer's Principle in a Feedback Trap, *Phys. Rev. Lett.* **113**, 190601 (2014).
- [20] K. Proesmans, J. Ehrich, and J. Bechhoefer, Finite-Time Landauer Principle, *Phys. Rev. Lett.* **125**, 100602 (2020).
- [21] K. Proesmans, J. Ehrich, and J. Bechhoefer, Optimal finite-time bit erasure under full control, *Phys. Rev. E* **102**, 032105 (2020).
- [22] K. Proesmans and J. Bechhoefer, Erasing a majority-logic bit, *Europhys. Lett.* **133**, 30002 (2021).
- [23] M. T. Woodside and S. M. Block, Reconstructing folding energy landscapes by single-molecule force spectroscopy, *Annu. Rev. Biophys.* **43**, 19 (2014).
- [24] J. Camunas-Soler, M. Ribezzi-Crivellari, and F. Ritort, Elastic properties of nucleic acids by single-molecule force spectroscopy, *Annu. Rev. Biophys.* **45**, 65 (2016).
- [25] S. Ciliberto, Experiments in Stochastic Thermodynamics: Short History and Perspectives, *Phys. Rev. X* **7**, 021051 (2017).
- [26] N. A. Sinitsyn and I. Nemenman, The berry phase and the pump flux in stochastic chemical kinetics, *Europhys. Lett.* **77**, 58001 (2007).
- [27] S. Rahav, J. Horowitz, and C. Jarzynski, Directed Flow in Nonadiabatic Stochastic Pumps, *Phys. Rev. Lett.* **101**, 140602 (2008).
- [28] V. Y. Chernyak and N. A. Sinitsyn, Pumping Restriction Theorem for Stochastic Networks, *Phys. Rev. Lett.* **101**, 160601 (2008).
- [29] X. Fang, K. Kruse, T. Lu, and J. Wang, Nonequilibrium physics in biology, *Rev. Mod. Phys.* **91**, 045004 (2019).
- [30] M. L. Mugnai, C. Hyeon, M. Hinczewski, and D. Thirumalai, Theoretical perspectives on biological machines, *Rev. Mod. Phys.* **92**, 025001 (2020).
- [31] E. Aurell, C. Mejía-Monasterio, and P. Muratore-Ginanneschi, Optimal Protocols and Optimal Transport in Stochastic Thermodynamics, *Phys. Rev. Lett.* **106**, 250601 (2011).
- [32] K. Gawedzki, Fluctuation relations in stochastic thermodynamics, [arXiv:1308.1518](https://arxiv.org/abs/1308.1518).
- [33] A. Dechant and Y. Sakurai, Thermodynamic interpretation of Wasserstein distance, [arXiv:1912.08405](https://arxiv.org/abs/1912.08405).
- [34] P. Muratore-Ginanneschi, C. Mejía-Monasterio, and L. Peliti, Heat release by controlled continuous-time Markov jump processes, *J. Stat. Phys.* **150**, 181 (2013).
- [35] U. Seifert, Stochastic thermodynamics, fluctuation theorems, and molecular machines, *Rep. Prog. Phys.* **75**, 126001 (2012).
- [36] See Supplemental Material at <http://link.aps.org/supplemental/10.1103/PhysRevE.103.L050105> for a discussion of the linear term of Eq. (11), a proof of the bounds Eqs. (21) and (23), and details on the numerical implementation, which includes Refs. [37,38].
- [37] R. Osada, T. Funkhouser, B. Chazelle, and D. Dobkin, Shape distributions, *ACM Trans. Graph.* **21**, 807 (2002).
- [38] M. Hanke-Bourgeois, *Grundlagen der Numerischen Mathematik und des Wissenschaftlichen Rechnens*, 3rd ed. (Vieweg + Teubner, Wiesbaden, Germany, 2009).